Journal of Power Sources 254 (2014) 126–136

Contents lists available at ScienceDirect

Journal of Power Sources

journal homepage: www.elsevier.com/locate/jpowsour

Fuel cell–gas turbine hybrid system design part II: Dynamics and control

Dustin McLarty, Jack Brouwer*, Scott Samuelsen

National Fuel Cell Research Center, University of California, Irvine, CA 92697, USA

HIGHLIGHTS

- Dynamics and controls development for fuel cell gas turbine (FC-GT) hybrid systems.
- Molten carbonate hybrid achieves 2:1 turndown at 66% efficiency (LHV) and 1.5 MW.
- Solid oxide hybrid achieves 4:1 turndown at 71% % efficiency (LHV) and 100 MW.
- Spatial temperature variation and surge margin are maintained during transients.
- Cascaded P–I controllers with feed-forward are utilized for hybrid system control.

ARTICLE INFO

Article history:
Received 13 August 2013
Received in revised form
25 November 2013
Accepted 29 November 2013
Available online 21 December 2013

Keywords:
Hybrid fuel cell gas turbine
Solid oxide fuel cell
Molten carbonate fuel cell
System design
Dynamics
Control

ABSTRACT

Fuel cell gas turbine hybrid systems have achieved ultra-high efficiency and ultra-low emissions at small scales, but have yet to demonstrate effective dynamic responsiveness or base-load cost savings. Fuel cell systems and hybrid prototypes have not utilized controls to address thermal cycling during load following operation, and have thus been relegated to the less valuable base-load and peak shaving power market. Additionally, pressurized hybrid topping cycles have exhibited increased stall/surge characteristics particularly during off-design operation. This paper evaluates additional control actuators with simple control methods capable of mitigating spatial temperature variation and stall/surge risk during load following operation of hybrid fuel cell systems. The novel use of detailed, spatially resolved, physical fuel cell and turbine models in an integrated system simulation enables the development and evaluation of these additional control methods. It is shown that the hybrid system can achieve greater dynamic response over a larger operating envelope than either individual sub-system; the fuel cell or gas turbine. Results indicate that a combined feed-forward, P–I and cascade control strategy is capable of handling moderate perturbations and achieving a 2:1 (MCFC) or 4:1 (SOFC) turndown ratio while retaining >65% fuel-to-electricity efficiency, while maintaining an acceptable stack temperature profile and stall/surge margin.

1. Introduction

Distributed energy resources can be characterized as intermittent, base-load, or load following power generation. Load following generators can meet building load dynamics, provide emergency or backup power, and support deployments of intermittent renewables; wind and solar. Flexible operation increases the value of a system which is otherwise non-competitive on a dollars per kilowatt-hour basis. Reciprocating engines and turbines operate in this space, but are subject fuel price volatility, part-load efficiency derate and stringent emission regulations in urban markets which require exhaust cleanup. A grid connected or distributed power resource can meet demand as either a base-loaded or load following resource. Base-loaded refers to constant power output operation, while load following operation can be scheduled, manually controlled or fully responsive to load power demand dynamics. The characteristics of the generator often determine the manner in which the resource is dispatched. Turbines have fast dynamic response characteristics amenable to part-load operation, but the drawbacks include reduced efficiency, increased emissions and flame instability. Most large turbines and many micro-turbines increase their operating range with staged combustion, but emissions can remain extremely high when some fuel injectors are disengaged at part load. Natural gas fired simple cycle turbines operate as load following

* Corresponding author. Tel.: +1 949 824 1999; fax: +1 949 824 7423.
E-mail addresses: jb@nfcrc.uci.edu, jb@apep.uci.edu, jbrouwer@uci.edu (J. Brouwer).

0378-7753/$ – see front matter © 2014 Elsevier B.V. All rights reserved.
http://dx.doi.org/10.1016/j.jpowsour.2013.11.123

Nomenclature

CHP	combined heat and power
DFC	direct fuel cell
FC	fuel cell
GT	gas turbine
IGV	inlet guide vane
MCFC	molten carbonate fuel cell
MTG	micro-turbine generator
NFCRC	national fuel cell research center
η	efficiency
P–I	proportional/integral control
SOFC	solid oxide fuel cell

"peaker" plants despite low efficiency and high emissions, while cleaner and more efficient combined cycle plants are increasingly operated continuously at rated capacity due to thermal integration of the turbine with the heat-recovery-steam-generation unit, the low price of natural gas, and the limited excess generating capacity on the grid [1]. Micro-turbines operate at the distributed resource scale providing base-load power, peak reduction through manual dispatch, or backup power. In backup power or grid independent applications micro-turbines are capable of meeting rapid load dynamics, albeit with low efficiency and moderate to severe emissions penalties for part-load operating conditions [2]. To-date, stationary fuel cells have only been deployed as a distributed resource and have typically been operated as base load generators. However, fuel cell systems have been shown to be capable of simultaneously achieving high efficiency and ultra-low emissions at full and part load conditions [3]. The two primary limitations on transient response are thermal integration with the natural gas fuel processor and stack-life deterioration due to thermal cycling [4]. The design of the hybrid systems studied herein address the fuel processing limitations while the controls outlined address the challenge of thermal cycling due to transient operation. Elimination of the turbine combustor in these hybrid configurations eliminates concerns of emissions and flame stability when part-loading the turbine. Due to the nature of fuel cell polarization curves, hybrid systems have the potential to have increased efficiency at part load. This paper will demonstrate how fuel-cell gas turbine hybrids are capable load following over a broad operating envelope without the efficiency, emissions, or stack-life tradeoffs of either individual system.

2. Background

Part I outlined the designs, demonstrations and potential applications of current state-of-the-art fuel cell and gas turbine technology [5,6]. This paper will focus on the off-design performance, dynamic operation and control of hybrid fuel cell gas turbine technology. The approach will emphasize minimizing thermal transients and temperature gradients within the planar fuel cell, sustaining sufficient stall/surge margin in the turbo-machinery, and maximizing part-load efficiency. Early experimental results and demonstration units [3,7] have highlighted the need for additional controls development, particularly for disturbance rejection [8] and off-design operation [9]. Test facilities employing a hardware-in-the-loop approach have been built in the United States [10] and Italy [11] to test various features of transient turbine operation, particularly start-up, shut-down, and the stall/surge phenomena [12]. Researchers in the Thermochemical Power Group have identified several distinct challenges of pressurized SOFC operation in particular the unstable behavior resulting from pressure transients in the cathode and anode compartments [13,14]. These real-world tests have required the development of simplified models applicable to real-time control [15,16].

Analysis suggests that both molten carbonate [17] and solid oxide [18] fuel cell gas turbine (FC-GT) hybrids could be capable of dynamic load following at ultra-high efficiency with the appropriate controls to sustain stack integrity and lifespan [4,19–22]. Control of internal temperature transients has been the focus of control strategies for stand-alone fuel cell systems [23] and hybrids [24]. Few measurements of internal temperature distributions are available in the literature [25], but modeling efforts have given important insights into the spatial temperature distributions [26] and impact on stack degradation and failure modes [20]. Many control studies have assumed overly simplified or non-physical dynamic models [27], and very few have models calibrated to or verified against experimental demonstrations [8]. A similar analysis of tubular SOFC-GT hybrids utilized a dual mode generator/motor in conjunction with a battery to improve transient load following in a small, 5 kW, transportation application which lacked any air flow control due to the small size [28]. Steady-state analyses offer insights into off-design performance with high turndown ratios, up to 5:1 [29], without considering the transient response and necessary control requirements. Proposed strategies for controlling stack air flow include variable speed turbines [30,31], variable inlet nozzle geometry [29], variable inlet guide vanes, variable flow ejectors [32], and bypass valves. SOFC-GT hybrids have been shown to exhibit high efficiency with turndown ratios of 5:1 [29]. Highly dynamic applications require manipulation of the cathode air flow rate through recirculation, bypass or variable mass flow turbomachinery [30–32].

The current study uses dynamic physical models based upon the first principles of mass and energy conservation, heat transfer, and chemical and electrochemical reactions as detailed in Refs. [8,26]. These models include a quasi-3D spatially resolved fuel cell model fully capable of simulating a variety of cell geometries and flow configurations, molten carbonate or solid oxide fuel cells with internal, indirect or external fuel reforming. The turbo-machinery model employs publicly available empirical performance maps for both radial and axial flow compressors and turbines. The turbo-machinery modeling tool is able to capture the design, off-design and transient performance of a simple cycle axial-flow turbine located at UC Irvine and several MTG units from different manufactures tested at the NFCRC as both stand-alone and hybrid systems. Both models capture transient response of the fuel reformation, electrochemistry, mass flow and heat transfer at physical time scales down to 0.01 s. The sensitivity was previously shown to well capture system transients caused by subtle perturbations in ambient temperature and pressure [8].

Initial market offerings of fuel cell technology have targeted specific regions with high electrical rates, strict emissions requirements, and/or energy and environmental policies that support fuel cell installation and operation. Diminishing fuel cell system capital and installation costs and supportive policies have made fuel cell systems economically attractive in some areas with only moderately high electrical rates. Fuel cell systems could become increasingly attractive if they could produce clean rapid load-following power that can meet dynamic loads and/or complement renewable intermittency. Dynamic load following fuel cell and hybrid FC-GT systems could produce more valuable dispatchable power, even competing with and replacing high emissions and low efficiency "peaker" plants.

3. Control development

3.1. System description

This paper will present the controls development for two FC-GT systems discussed in Part I. The first system modeled is the coal syngas fueled SOFC-GT topping cycle, which integrates an SOFC system pressurized to 10 atm with an axial flow turbine. The turbine in this cycle does not achieve nominal firing temperature, is constrained to constant speed operation, and employs inlet guide vanes capable of reducing nominal air flow by up to 40%. The fuel cell pressure loss is nominally 50 kPa and the cathode flow recirculation amount is found to be 16% for steady state design conditions, which is driven by an electrically powered blower with a performance map similar to a single stage radial compressor. The blower is sized to meet 120% of the nominal recirculation flow and the rotational inertia is scaled proportional to its size. The blower efficiency map is considered in calculation of the parasitic load and amounts to ~1% of the net system output. Nominally this system achieves 73.7% fuel to electric efficiency.

The second system is an MCFC bottoming cycle combining a FCE DFC1500® and a Capstone C250® as detailed in Part I of this paper. The integration of the two sub-systems required operation of the fuel cell substantially off-design, but resulted in a hybrid efficiency of 74.4%. The operating envelope of this FC-GT hybrid is small because the turbine sub-system is undersized for this fuel cell. The addition of a blower which supplements the turbine exhaust has a moderate impact on efficiency; the system achieves 66.0% efficiency (LHV) at 1.5 MW. The blower allows for operation of the DFC1500® near design conditions and increases the operating envelope of the hybrid by increasing the controllable range of air flow rate that can be provided to the cathode. The blower incorporates an additional actuator for controlling the cathode inlet temperature with a dilution air stream. Atmospheric operation of the fuel cell allows the inclusion of a supplemental blower at this location in the cycle. Fig. 4 provides a schematic layout of this MCFC–GT hybrid.

3.2. Fuel cell and turbine control

Both fuel cells and gas turbines have a number of variable parameters that allow them to be controlled over a range of power output. For the fuel cell these include the air flow rate, the fuel flow rate, the stack voltage/current, and the operating temperature. The flow rates and stack voltage/current are manipulated to maintain fixed temperature operation during both steady and transient operation in order to minimize thermal stress and degradation of the stack. Stack voltage and current are directly linked through the electrochemical performance of the fuel cell. This paper will utilize current control rather than voltage control because it is positively correlated with both power and fuel use at constant fuel utilization. A suitable voltage controller could be used interchangeably with the current controller in this work. Fuel flow will be manipulated to control both stack power and temperature. The majority of the fuel will be directly proportional to the current in order to maintain fixed fuel utilization. Additional fuel will be added in order to increase or decrease the total fuel cell heating and will be referred to as pre-FC fuel injection. Air flow in a fuel cell system is provided by a blower which can be highly responsive over a wide range of outputs. The response of the blower is limited by rotational inertia as it spins up.

Gas turbines can operate of a range of power by controlling both fuel and air flow. Large axial flow turbines control air flow with variable inlet guide vanes and compressor bleed. Variable inlet guide vanes alter the apparent angle of attack for the first 6–8 stator stages to reduce the nominal flow rate while maintaining high compression and thus high efficiency at part load. There is still a considerable reduction in the efficiency, particularly for non-recuperated single cycle gas turbines. Compressor bleed is typically used only during start-up and shut-down to avoid compressor stall/surge. The rotational speed of a gas turbine is controlled by the generator load. Micro-turbine generators (MTG) utilize radial compressors, and cannot apply the same variable guide vane techniques. The power output, typically on the scale of 30–300 kW, allows the rotational speed of the micro turbine to be asynchronous with the grid. Reducing the rotational speed at part-load maintains a higher combustion temperature, but reduces the operating pressure and efficiency of the engine. The range of air flow reduction from inlet guide vanes is typically small, ~30%, while the reduction in rotational speed of a MTG can control air flow over a larger range, ~50%. This work will demonstrate inlet guide vane control for the SOC-GT system and speed control for the MCFC–GT system. Compressor bleed will be used in some particular instances to increase the stall/surge margin of large systems under specific operating conditions.

The fuel flow control of a turbine is a simple as manipulating the fuel injection into the combustor. In a well-designed FC-GT hybrid the total fuel cell heating completely replaces the total combustion heating. That is the heat given off by the fuel cell and the oxidation of anode off-gas provide all of the thermal energy needed to drive the turbine. However, under part load conditions the total fuel cell heating decreases while the total combustion heating necessary does not. Thus it is beneficial to retain the combustor when the gas turbine and fuel cell are integrated into a hybrid system. Injecting fuel into the combustor supplements the total fuel cell heating by injecting heat immediately upstream of the turbine.

3.3. SOFC-GT hybrid control

Additional actuators can be added when the fuel cell and gas turbine sub-systems are integrated. These include bypass valves which can redirect air flow around heat exchangers or the fuel cell. The SOFC-GT cycle analyzed with the additional bypass loops is shown in Fig. 1.

To operate a FC-GT at part load the control strategy must include at a minimum a power controller to manipulate the fuel cell stack current, a fuel controller to maintain fixed fuel utilization as current fluctuates, and a generator load controller to maintain the rotational speed of the turbine. This combination of power, fuel, and speed control will be considered the baseline control scenario onto which additional controllers will be added. The additional controls evaluated will be the following; a) Post-FC fuel injection, b) Pre-FC fuel injection, c) inlet guide vane control with blower recirculation

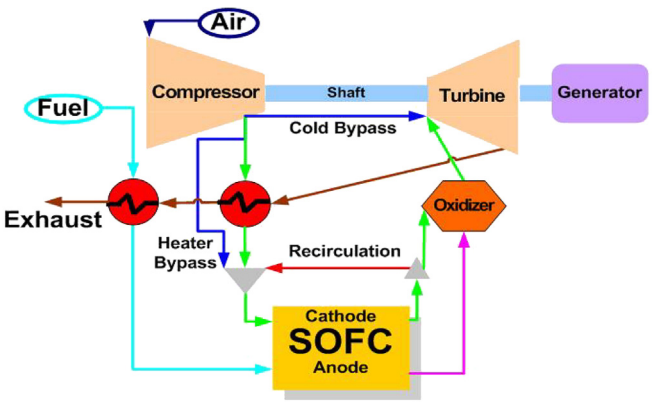

Fig. 1. SOFC-GT hybrid with cathode recirculation and fuel cell bypass control loops.

control, and d) FC air bypass with blower recirculation control. In each controller the feedback error, $e(t)$, is normalized by the set point, $r(t)$, before passing through the PI controller with the appropriate gain values detailed in Table 2 (Fig. 2).

Post-FC fuel injection corresponds to combusting additional fuel in the combustor of the gas turbine. This method can supplement the total fuel cell heating at part load or full load to ensure the turbine is operated within its design envelope. If the turbine is over-sized for the fuel cell, this type of supplementary combustor firing is necessary to enable integration of the two sub-systems. This control strategy presented in Section 4.2 will have the largest impact on system efficiency.

A similar control strategy injects extra fuel into the fuel cell. The current- based fuel controller also manipulates the fuel flow, so upstream fuel injection does not require any additional actuators. This pre-FC fuel injection, discussed in Section 4.2, also increases the total fuel cell heating at part load, but unlike post-FC fuel injection, this strategy improves the efficiency of the FC by increasing the available hydrogen throughout the anode chamber. The FC-GT system efficiency is substantially reduced as in post-FC fuel injection, albeit by a smaller amount.

Under part-load operation of a FC-GT hybrid the total fuel cell heating is reduced. To sustain high operating efficiency it would be preferable to reduce the total combustion heating by an equal amount through a reduction in air flow rate. This would avoid the efficiency penalty of either pre- or post-FC fuel injection. In large systems air flow can be reduced with the application of variable inlet guide vanes. Air flow can also be manipulated using recirculation or bypass loops. Part I demonstrated that the specific fuel cell heating of pressurized SOFC technology operated on syngas is much less than the specific combustion heating of large turbine systems, and that cathode recirculation was the most efficient means of bridging the gap. If recirculation is already built into the hybrid design it is reasonable to treat the amount of recirculation as an additional actuator. Air flow control with a combination of inlet guide vane and recirculation will be discussed in Section 4.3. The range of air flow control from inlet guide vane manipulation is small. Greater reductions in cathode air flow at part load can be achieved with the addition of a bypass valve which redirects some compressor exhaust directly to the turbine rather than the cathode. Bypassing air from the compressor exhaust requires a high temperature, high pressure valve which can introduce substantial flow control or pressure oscillation challenges in a real system. These can be mitigated with slow actuation of the bypass valve. Air flow control using fuel cell bypass and cathode recirculation is detailed in Section 4.4.

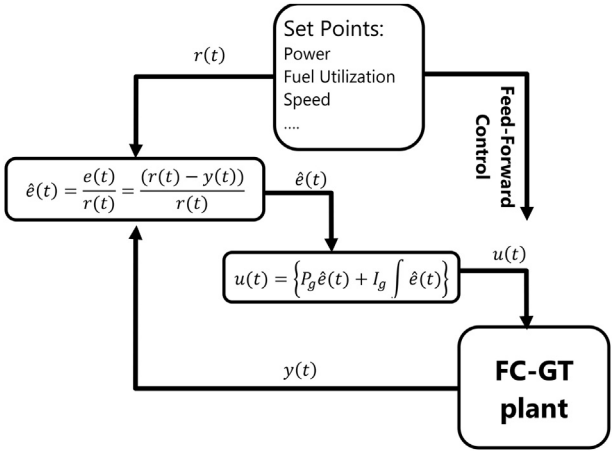

Fig. 2. P–I feedback control loops for FC-GT control.

3.4. Integrated FC-GT control strategy

Each of the four supplemental control strategies has its own benefits and drawbacks. The operating envelope of the FC-GT hybrid is different with each strategy. Integrating all four of these control strategies can combine the best attributes of each; the high efficiency of inlet guide vane manipulation, the quick responsiveness of post-FC fuel injection, and the wide range of fuel cell bypass. These control strategies are capable of accommodating a reduction of power from the fuel cell stack, when the total fuel cell heating becomes less than the total combustion heating. This assumes the nominal condition of the FC-GT hybrid corresponds to the maximum power. If the power were to increase the additional total fuel cell heating would need to be rejected in the exhaust. This is possible with the addition of a recuperator bypass which diverts hot turbine exhaust gases away from the cathode pre-heater.

The addition of recuperator bypass serves to lower the premixing cathode inlet temperature at full load on hot days. Used in conjunction with blower recirculation controlling post-mixed cathode inlet temperature, this bypass valve can increase air flow through the stack for a given cathode inlet temperature and power set point condition. Recuperator bypass control will be applied as the opposite of fuel cell bypass with the same controller and could be implemented with co-located valves. This bypass also accommodates ambient temperature deviations above the design case when operating at full load. It will be shown in Section 4.5 how the daily peak in electricity demand, coincident with the daily peak temperature, requires the hybrid to divert hot exhaust gas away from the recuperator to maintain the stack operating temperature. The integrated control strategy, outlined in Fig. 3, measures five system states and uses five controllers to actuate three air valves, two fuel valves, the inlet guide vane angle, the generator load, and the fuel cell current. The feed-forward controls applied to the inlet guide vane and fuel cell bypass control are described in Equations (1) and (2) respectively.

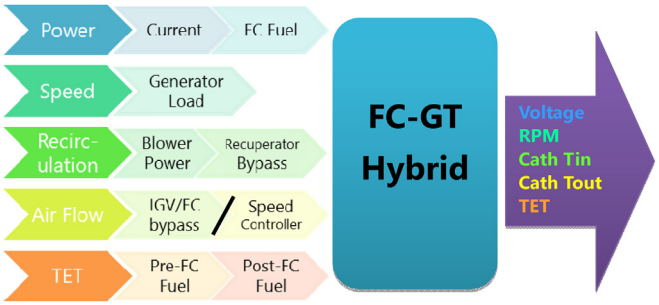

Fig. 3. Control overview for synchronous SOFC-GT topping cycle with IGV and bypass.

$$\mathrm{IGV_{FF}} = \left(G_{\mathrm{IGV\_FF}}\left(1 - \frac{\dot{W}_{\mathrm{demand}}}{\dot{W}_{\mathrm{nominal}}}\right)\right)^{3/4} \times 100 + \mathrm{IGV_{initial}} \quad (1)$$

$$\mathrm{FC\_By_{FF}} = \left(G_{\mathrm{FC\_By\_FF}}\left(1 - \frac{\dot{W}_{\mathrm{demand}}}{\dot{W}_{\mathrm{nominal}}}\right)\right)^{.813} + \mathrm{FC\_By_{initial}} - .5\frac{\mathrm{IGV_{FF}}}{100} \quad (2)$$

Tightening the controls to reduce transient impacts and avoiding feed-back instability requires a few modifications to the simple PI controllers introduced previously. The improvements include anti-windup on all integral controllers, exponential feed-forward control for inlet guide vane and fuel cell bypass control, variable integral and proportional gain values for fuel cell bypass control, and communication between controllers. Table 1 presents a summary of the control parameters. Each feed-back error is normalized making the integral gains roughly inversely proportional to the time-scale of response. A cascade controller is used to control system power output with the first controller using the synchronous generator output to determine the proportion of total power generated by the FC, and the second integrator determining the fuel cell current. This combined controller approach with feed-forward control is capable of substantially rapid load following at high efficiency.

3.5. MCFC–MTG Hybrid control

At the distributed generation scale similar control approaches are applied to the smaller scale FC-GT system. Identical baseline controllers maintain power, fuel flow rate, and turbine speed. Moderate temperature bypass valves were considered at two locations in the design. The first location, immediately downstream of the compressor, bypasses compressor exhaust directly to the turbine inlet. This bypass pathway was tested as an independent control, but was not utilized in the integrated control strategy. The second location is immediately downstream of the turbine, which serves two purposes: (1) to bypass the anode oxidizer and secondary heat recovery unit and direct turbine exhaust to the cathode, and (2) bleeds turbine exhaust to expel excess air. Under the test conditions shown the option to bleed turbine exhaust was never exercised, but it would be utilized during ultra-low power operation and during start-up or shut-down. The available controllers, pre/post fuel injection, bypass, or speed control, can prioritize either cathode inlet or outlet temperature. Slow thermal transient response of the cathode outlet temperature suggests that inlet temperature control would be less likely to introduce non-minimum phase behavior. In the integrated controller strategy it was decided to apply a look-up table to the cathode inlet temperature set-point, which aims to maintain the spatially averaged electrolyte temperature near nominal operating conditions. A schematic diagram of this MCFC–GT hybrid can be seen in Fig. 4.

The indirect internal reforming of the DFC1500® design provides the majority of stack cooling, particularly at lower power density operation. The air flow necessary at part load to maintain stack cooling is less than that required for the syngas fueled SOFC. Thus, the same load shed perturbation requires a greater range of air flow adjustment in the MCFC–GT system, and has a more detrimental impact on the surge margin. Stall/surge severely limits the ability of

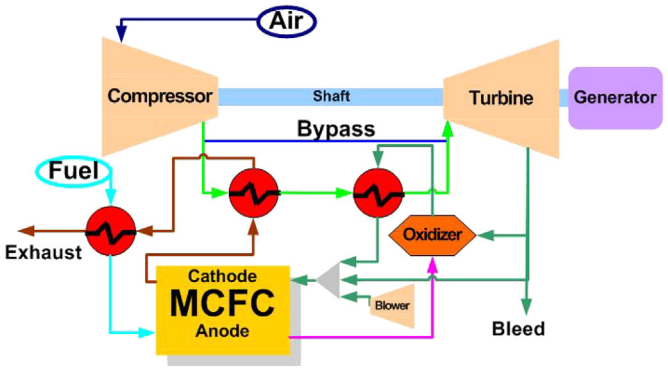

Fig. 4. MCFC–MTG hybrid with supplemental blower, turbine bleed and fuel cell bypass.

speed control to adjust air flow rate during part load operation of the current MCFC–MTG bottoming cycle. Table 2 lists the control gain parameters used for control of the MCFC–MTG bottoming cycle. The lower power density operation of an MCFC (compared to an SOFC) results in slow thermal transients, even at the distributed generation scale, once again requiring feed-forward control of the cathode exhaust temperature, as shown in Equations (3) and (4).

$$\mathrm{Speed}_{\mathrm{FF}} = \left(G_{\mathrm{speed\_FF}}\left(1-\frac{\dot{W}_{\mathrm{demand}}}{\dot{W}_{\mathrm{nominal}}}\right)\right)^{3/4} \times (-.35) \tag{3}$$

$$\mathrm{FC\_By}_{\mathrm{FF}} = \left(G_{\mathrm{FC\_By\_FF}}\left(1-\frac{\dot{W}_{\mathrm{demand}}}{\dot{W}_{\mathrm{nominal}}}\right)\right)^{1} - \frac{\mathrm{RPM}_{\mathrm{des}}-\mathrm{RPM}}{\mathrm{RPM}_{\mathrm{des}}} \tag{4}$$

4. Multi-MW hybrid control with synchronous generator

To test these control strategies, all five control techniques were subjected to a load shed perturbation down to 70% load and subsequently tested for dynamic load following of a typical campus load profile, using a measured load profile from the UC Irvine campus for two disparate summer days (one much hotter than the other). The UC Irvine campus load varies diurnally from 62% to 100% of peak load with a daily peak at about 2 PM; coincident with the peak ambient temperature. The campus electric load demand, measured at 15 min intervals, ranged from 13 MW to a peak of 19 MW. All five control strategies were able to control the SOFC-GT system to successfully meet the campus dynamic load profile and the load shed perturbations with varying average efficiency and stack temperature deviations, as shown in Table 3.

Table 1
Controller gain specifications for integrated control strategy of SOFC-GT topping cycle.

State	Actuator	Integral gain	Proportional gain	Feed-forward gain
Net power	Current	1.0e-2, 1e-1	0.0	0.0
Turbine speed	Generator Load	5.0e-1	1.0e2	0.0
Cathode inlet temperature	Blower power/ Heater bypass	5.0e-2	4.0	0.0
Cathode exhaust temperature	Guide vane angle (IGV) or Bypass (By)	0.0 (IGV) 1e-3(By)	1.0 (IGV) 2.0 (By)	0.7 (IGV) 1.16 (By)
Turbine exhaust temperature	Pre-FC fuel or post-FC fuel	5.0e-2 (Pre-) 1.0e-4 (Post)	0.0	0.0

Table 2
Controller gain specifications for MCFC–MTG control strategy.

State	Actuator	Integral gain	Proportional gain	Feed-forward gain
Net power	Current	1.0e-1, 1e0	0.0	0.0
Turbine speed	Generator load	5.0e-1	1.0	0.7
Cathode inlet temperature	Blower power/ Oxidizer bypass	2.0e-2	4.0	0.0
Cathode exhaust temperature	Bypass valve	1e-2	1	0.7
Turbine exhaust temperature	Pre-FC fuel or post-FC fuel	0.0 (Pre-) 1.0e-3 (Post)	0.0	0.0

Table 3
Summary of system efficiency for different control methods, for the FC-GT system that nominally achieves 73.7% fuel-to-electricity conversion efficiency.

Control method	Efficiency @70% load	Cathode inlet/ outlet (Δ°C)	48 h Average efficiency	Transient cathode inlet/ outlet (±°C)
No control	70.2	−71.2, −91.5	70.9	66.5, 75.8
Pre-FC fuel	62.4	−13.6, −113.8	65.3	27.8, 98.5
Post-FC Fuel	65.4	−1.2, −88.0	67.4	10.4, 60.0
Guide vane	72.1	−0.1, −1.4	72.4	1.7, 20.4
FC Bypass	71.5	0.0, −0.4	71.9	0.2, 10.4
Combined	72.0	0.0, 0.0	71.1	0.8, 9.3

4.1. Baseline control & response

The FC-GT model is constructed with the baseline power, fuel, and speed controllers outlined previously and subjected to several transient perturbations. The first perturbation is a load shed to 90% nominal power, followed by a second load shed to 70% of nominal power. The response of the hybrid system is shown in Fig. 5. The system responses of greatest concern for short or long-term failure modes are the stack operating temperature, planar thermal gradient, and surge margin. Operating temperature and current density are relevant to long-term voltage degradation. Thermal gradient is an indicator of thermal stress, which could cause fracture and immediate failure, and electrolyte loss (MCFC) and electrochemical loss distributions, which must be maintained within an acceptable range. Surge margin, a measure of the susceptibility of the compressor to stall/surge, is of particular concern in a pressurized topping cycle due to the additional pressure loss and large volume introduced between the compressor and turbine. The additional mass storage delays pressure response during dynamic operation and can lead to sudden and irrecoverable loss of air flow.

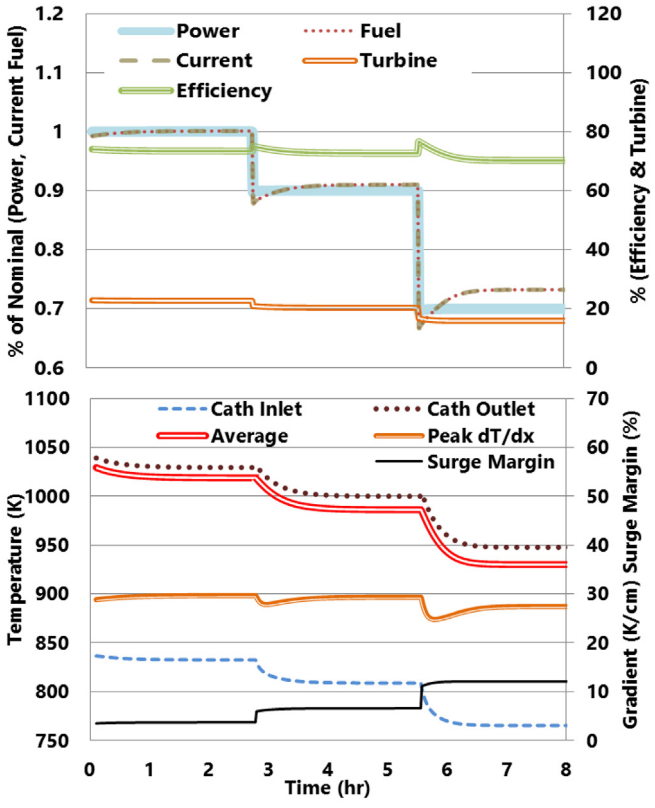

Fig. 5. Transient response to 10%, 20% load shed with baseline controls.

The initial response to the load perturbation is a current reduction. Fuel input is manipulated in proportion to current to maintain a fixed 80% fuel utilization. Initially voltage rises at the reduced current level, but the reduced heat generation and nearly constant air flow steadily reduce the stack temperature until voltage decreases and the heat is partially recovered, as seen in Fig. 5. The reduced specific fuel cell heating at lower load conditions (90% and 70%) lowers the turbine inlet temperature, reducing system pressure and increasing the mass flow supplied by the compressor. Overall system efficiency diminishes from 73.7% to 70.2%, but the >70 °C drop in stack inlet temperature is likely unsustainable. The reduced stack temperature leads to a corresponding reduction in turbine inlet temperature, hence the increased surge margin. The small step rise in efficiency seen immediately after each load shed perturbation is a result of temporarily increased stack voltage due to the temporary maintenance of average temperatures that are higher than steady state conditions. This temporary rise in efficiency during a load shed indicates the potential for high efficiency part-load operation, but the balance of plant must effectively adjust to the different fuel cell performance characteristics associated with each of the various part-load operating conditions.

4.2. Pre-FC and post-FC fuel injection control

The first and second supplemental controllers discussed previously inject fuel either into a combustor upstream of the turbine or into the fuel cell itself. Controlling the turbine exhaust temperature is a typical control strategy that works well for operating a turbine at part-load conditions, and is a strategy potentially transferable to hybrid systems. This example uses supplemental fuel injection to control cathode inlet temperature because maintaining fixed stack temperature is more critical than maintaining fixed turbine temperature. In a hybrid system supplemental oxidation of fuel can recover the reduced total fuel cell heating at part-load and maintain cathode inlet temperature at fixed air flow. The additional fuel is oxidized with the anode tail gas or in a combustor.

Injecting supplemental fuel into the anode tail gas oxidizer or a downstream combustor maintains the power output of the turbine during system turn-down, as seen in Fig. 6. Maintaining a higher turbine inlet temperature ensures that recuperator effectiveness and cathode inlet temperature remains steady. The fuel cell power reduction is greater than in the un-controlled turn-down case due to the constant power output from the turbine. Current decreases more than power output as voltage increases by 20%. The reduced specific fuel cell heating lowers the cathode exhaust temperature by 88.0 °C and reduces thermal gradients by 50%, as seen in Fig. 6. To compensate for the reduced inlet preheating from cathode recirculation the turbine exhaust temperature is increased, which raises system pressure and reduces the surge margin. Net system efficiency is reduced from 73.7% to 62.5%.

The system responds very similarly to fuel injection upstream of the anode. This strategy amounts to changing the proportional relationship between current and fuel flow; effectively lowering fuel utilization at part load. There is some benefit to the system efficiency associated with higher Nernst potential and reduced activation and concentration losses due to the higher hydrogen concentration in the anode, but it does not address the unsustainable reduction in stack temperature. The improved stack voltage results in a smaller efficiency loss from 73.7% to 65.4% at 70% part load operation. Once again, the exhaust temperature and pressure rise, which reduces the operating surge margin. The impact on surge margin is 50% less than the post-FC fuel injection.

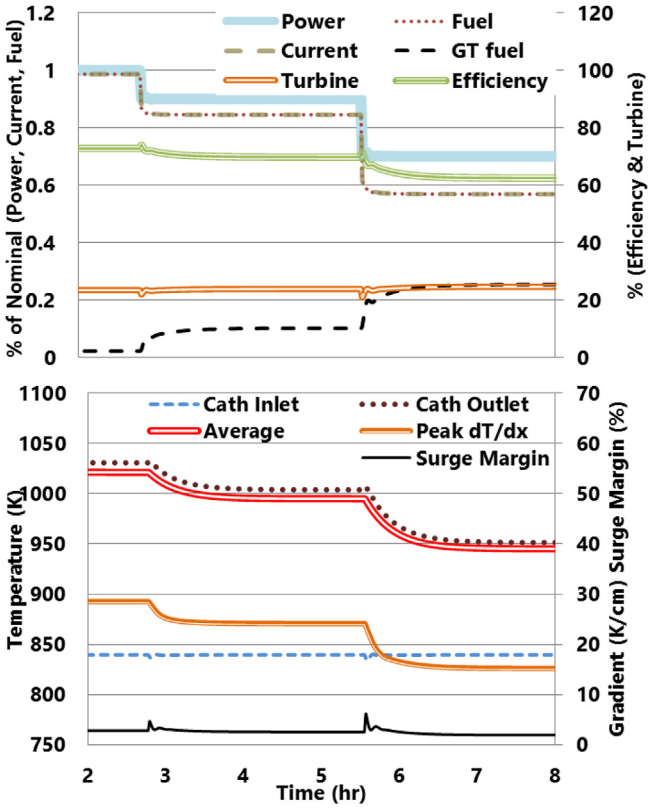

Fig. 6. Transient response to load shed with baseline controllers and post-FC fuel injection.

4.3. Inlet guide vane control

The first air flow control strategy outlined previously was the application of inlet guide vane manipulation employed in conjunction with variable cathode recirculation using blower power manipulation. This strategy reduces both fuel cell and turbine air flow at part load and maintains cathode inlet, cathode outlet, and turbine exhaust temperature. The inlet guide vane and blower dynamics are much quicker than the thermal transients of the stack, thus simple P–I feedback can effectively control the cathode inlet temperature. Both actuators manipulate the stack air flow and thus the net temperature rise across the stack. The typically long time-scale associated with thermal transients of SOFC and MCFC stacks, on the order of hours, introduces an instability shown in Fig. 7. At hour seven, the instability reaches the minimum threshold for stall/surge margin and a secondary control loop in the turbine model overrides the inlet guide vane command to recover the turbine operation. The inlet guide vane approach is capable of maintaining the fuel cell spatial temperature profile, but should be implemented with a feed-forward or MIMO controls approach. The simulation shown in Fig. 7 begins with a larger surge margin as a result of a small amount of compressor bleed. Compressor bleed can be used to mitigate the stall/surge risk when inlet guide vane actuation is applied. Compressor bleed was not utilized in this example to illustrate the impact of the hybrid system load shed on stall/surge risk. Compressor bleed is not a suitable solution to this issue since its range is limited and the impact on turbine efficiency is large.

In response to the initial load shed perturbation to 90% load the fuel cell temperature is maintained within 10 °C of nominal conditions despite control oscillations. Reduced stack current leads to increased stack voltage and efficiency. The higher efficiency and lower power reduces total fuel cell heating and triggers the inlet guide vanes to constrict air flow. Inlet guide vane manipulation, if applied in a feed-forward manner, provides the smallest reduction in efficiency from 73.7% to 72.1% fuel to electric efficiency at 70% load.

4.4. Fuel cell air bypass

The final control approach applied manipulates the stack air flow only. Bypassing compressor air around the fuel cell and directly to the turbine requires a high temperature valve, which can introduce additional pressure and heat losses, flow irregularities, and maintenance challenges. The hybrid system responses to the same load shed perturbations are similar to those observed for the inlet guide vane control scenario. The turbine response is less than with inlet guide vane control, and thus the instability is reduced, though still noticeable for the reduction to 70% load. The decreased turbine output lowers efficiency 2.2% points rather than the 1.6 seen with inlet guide vanes. Unlike the inlet guide vane control case, surge margin is increased at part load, and the range of controllability is large; bypass was opened 50% for a 30% load shed, indicating a >60% load shed is potentially possible with fuel cell air bypass control. Cathode recirculation increases but blower parasitic load decreases due to the reduced cathode flow and pressure loss.

4.5. Dynamic load following and 4:1 turn-down

In addition to the simple load shed test illustrated previously, each control strategy was tested for a simulated 48 h of the UC Irvine campus electric load profile, ranging from 13 to 19 MW. The

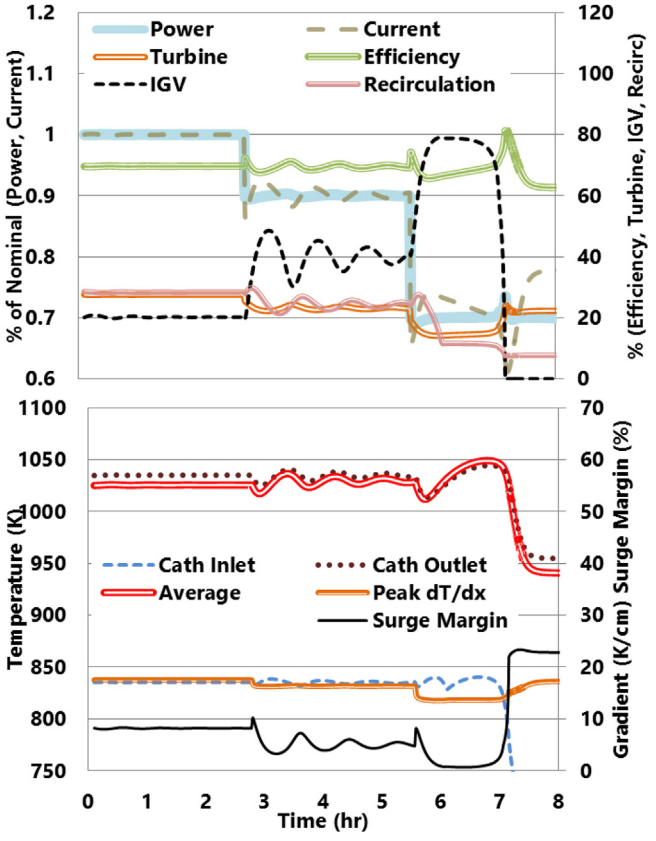

Fig. 7. Transient response to load shed with air flow control via IGV and blower manipulation.

baseline and supplemental control methods outlined effectively operated the system between 70% and 100% of rated capacity with varying impacts on efficiency and fuel cell temperature. Table 3 summarizes the efficiency penalties and stack temperature perturbations associated with each control strategy for the simple load shed and the 48 h campus load simulation.

Next the SOFC-GT was shrunk by 50% and paired with 10 MW of base load generation. This scenario doubles the dynamic range of the electric load that must be met by the dynamic dispatch of the hybrid FC-GT system, requiring a turndown to 30% of rated power. None of the individual control strategies were capable of achieving this 4:1 turndown. However, an integration of these control approaches into a single strategy which balances efficiency and range was able to handle the large turndown and rapid dynamic perturbations with minimal impact to stack temperature, thermal stress and compressor stall/surge margin Fig. 8 illustrates the system and controls response to the 48-h load transient. The system in operation achieves a peak efficiency of 73.7%, a minimum of 56.7% and an average efficiency of 67.4% over the 48 h period. Cathode inlet and exhaust are maintained within 1 °C and 13 °C respectively. The turbine inlet and exhaust recovery are significantly impacted at part load operation and responsible for the majority of the performance de-rate. Simple P–I and feed-forward control techniques can operate a well-designed hybrid FC-GT across a large operating envelope and effectively manage the rapid load transients expected at the multi-MW scale.

5. Sub-MW hybrid control with asynchronous generation

5.1. Baseline control & response

The MCFC–MTG hybrid system of Fig. 4 was subjected to the same load shed and 48-h campus load profile as the SOFC-GT system. The campus load profile was scaled to the 1.5 MW capacity of the FCE-DFC1500® and Capstone Turbine C-250 hybrid system outlined previously. The nominal stack temperature response was similar to that of the SOFC for the different control strategies, pre- and post-anode fuel injection and cathode bypass. These responses are summarized in Table 4, but not presented in graphs for brevity. The micro-turbine uses speed control rather than inlet guide vanes to manipulate air flow. Results from using speed control only, in conjunction with control of the supplemental blower, are presented below.

5.2. Speed control

The hybrid MCFC–MTG in this configuration nominally produces 1.55 MW at 64.5% fuel-to-electric efficiency. The fuel cell nominally produces 1.4 MW, the turbine produces 163 kW, and the blower consumes 13 kW. This particular cycle actually achieves higher efficiency under reduced load conditions since the voltage increase at part load more than offsets the turbine de-rate. At approximately 70% load the system no longer requires supplemental blower air injection to meet the stack cooling demands. The reduced output power operating state thus achieves 69.3% fuel-to-electric efficiency due in part to the eliminated parasitic load and the increased FC voltage. This part-load condition closely matches the optimal theoretical integration described in Part I using only the performance maps.

Immediately after the step reduction in power the rotational inertia of the turbo-machinery temporarily increases the generator output while the turbine speed controller acts to reach a reduced speed operating condition. This explains the temporary overshoots in current reduction and corresponding spikes in efficiency seen in Fig. 9. Air flow rate control, achieved with a combination of blower and turbine speed manipulation, maintains nearly fixed cathode inlet temperature mitigates exhaust temperature reduction to 30 °C at part load. The peak temperature gradient is reduced as a result of the lower current density and reduced endothermic methane reformation occurring in the imbedded reformer channels. Maintaining fixed cathode inlet temperature maintains near constant turbine exhaust temperature. Since this strategy is typical of micro-

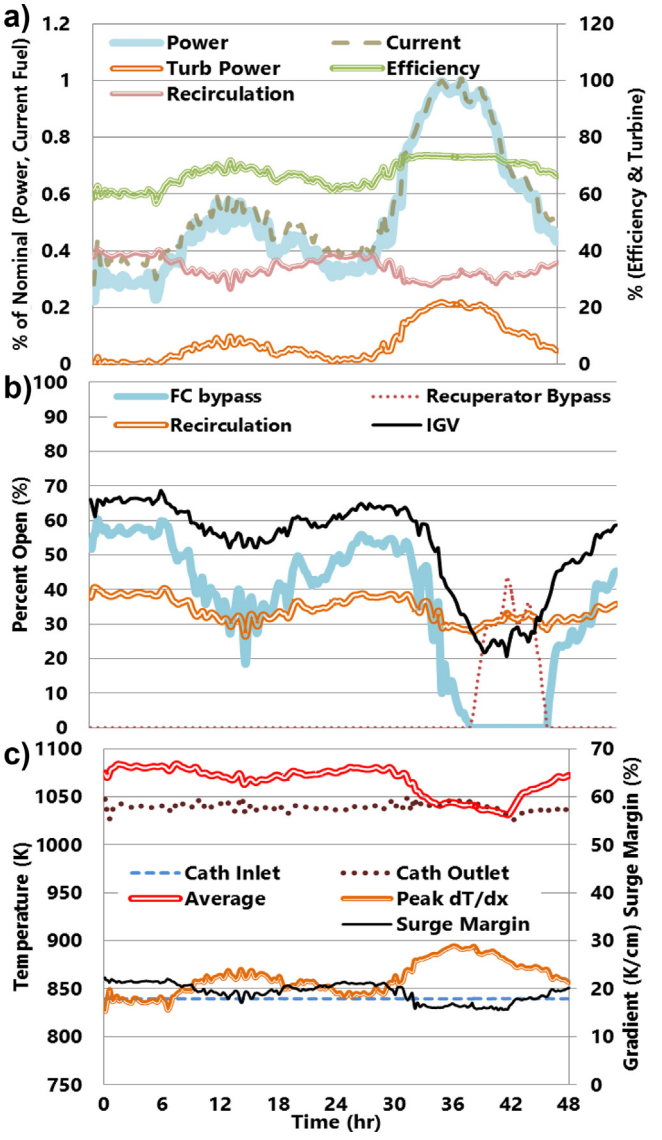

Fig. 8. Responses to a 48-h dynamic load profile ranging from 3 to 10 MW using the integrated control strategy a) system power and efficiency b) control actuation c) turbo-machinery and FC temperature.

Table 4
Summary of MCFC–MTG efficiency for different control methods, nominally 66.0%.

Control method	Efficiency @70% load	Electrolyte average ΔT (°C)	48 h Average efficiency	Electrolyte average $\pm\Delta T$ (°C)
No control	69.0	−81.2	N/A	N/A
Pre-FC fuel	70.9	−12.4	N/A	N/A
Post-FC fuel	64.7	−12.4	N/A	N/A
Speed control	69.2	−1.4	67.0	2.4
FC bypass	69.9	−6.5	62.0	13.1
Combined	70.6	−5.2	66.7	12.9

turbine part-load operation, the reduction in surge margin at reduced rotational speed is typical for part-load operation of the micro-turbine.

5.3. Integrated control strategy

Three of the four control strategies, post-FC fuel injection, speed control and FC bypass were integrated into a combined control strategy. Pre-FC fuel injection was not included since the impact on cell performance and lifespan of MCFC technology from operating at variable fuel utilization remains uncertain. The integrated control strategy could readily meet the scaled campus demand profile while achieving an average operating efficiency of 66.7%. Neither turbine speed, nor blower power, nor bypass actuators reach saturation, indicating that the controllable range is substantially greater than the 35% turndown, but the MCFC–MTG hybrid could not match the 4:1 turndown ratio of the SOFC-GT system. The system response and control actuation during the 48-h transient test is shown in Fig. 10. The electrolyte temperature was maintained within 13 °C of nominal operating conditions throughout the entire test.

The surge margin is typically larger in a radial flow micro-turbine because the range of pressurization across a single stage is much greater, and the peak compression efficiency is further from the stall pressure. This benefits the micro-turbine during hybridization when an additional heat exchanger downstream of the compressor substantially increases the pressure drop, and during speed turndown (both conditions that reduce surge margin). During a micro-turbine load shed perturbation, pressure decreases faster than turbine inlet temperature, resulting in lower air density at the turbine inlet and less mass flow expelled from the turbine. This drives the compressor operation towards stall/surge at part-load. The surge margin can be seen to decrease to below 10% when the turbine output drops below 80 kW. The likelihood of surge would continue to increase as the turbine is further unloaded and could not be recovered using high pressure bleed as was the case for a large axial-flow turbine. Minimizing the additional pressure drop caused by the second high pressure heat exchanger is critical to ensuring a wide range of operation in a hybrid system. Nonetheless, the dynamic performance achieved for this highly dynamic load profile is impressive, both avoiding surge and maintaining FC operating conditions within an acceptable range.

The increase in surge margin is inversely related to the turbine exhaust temperature. This relationship suggests maintaining a higher speed and thus higher air flow at part load might be able to produce a larger surge margin. The drawbacks of this approach would be reduced system efficiency and a further reduction in the temperature differential from cathode inlet to exit. Depending upon the impact that thermal cycling would have upon the MCFC performance and degradation characteristics, this approach could become an appropriate strategy for higher turn-down ratio operation.

5.4. Spatially resolved temperature perturbations

The dynamic simulations presented were conducted with a quasi-3D fuel cell model developed at the NFCRC. A spatial

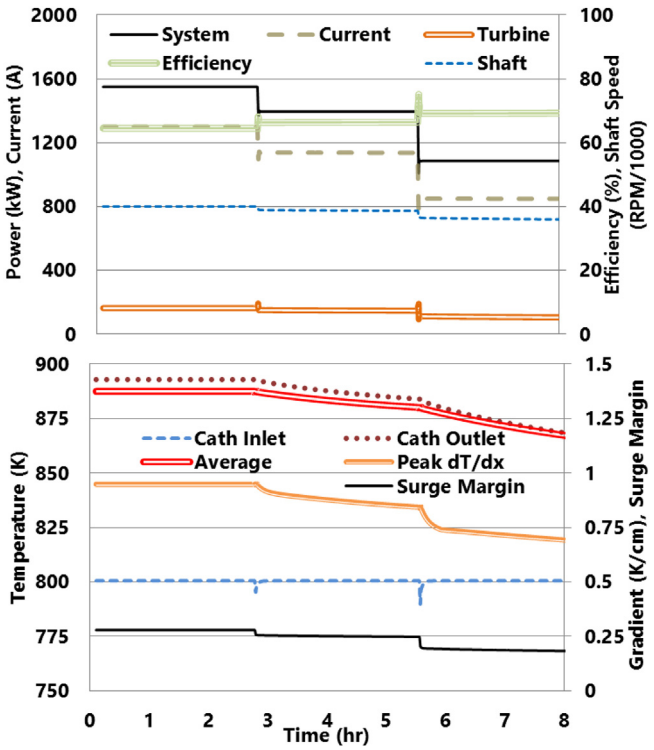

Fig. 9. Hybrid FCE DFC1500®/Capstone C250® (MCFC–MTG) response to load shed with baseline controllers and turbine speed control.

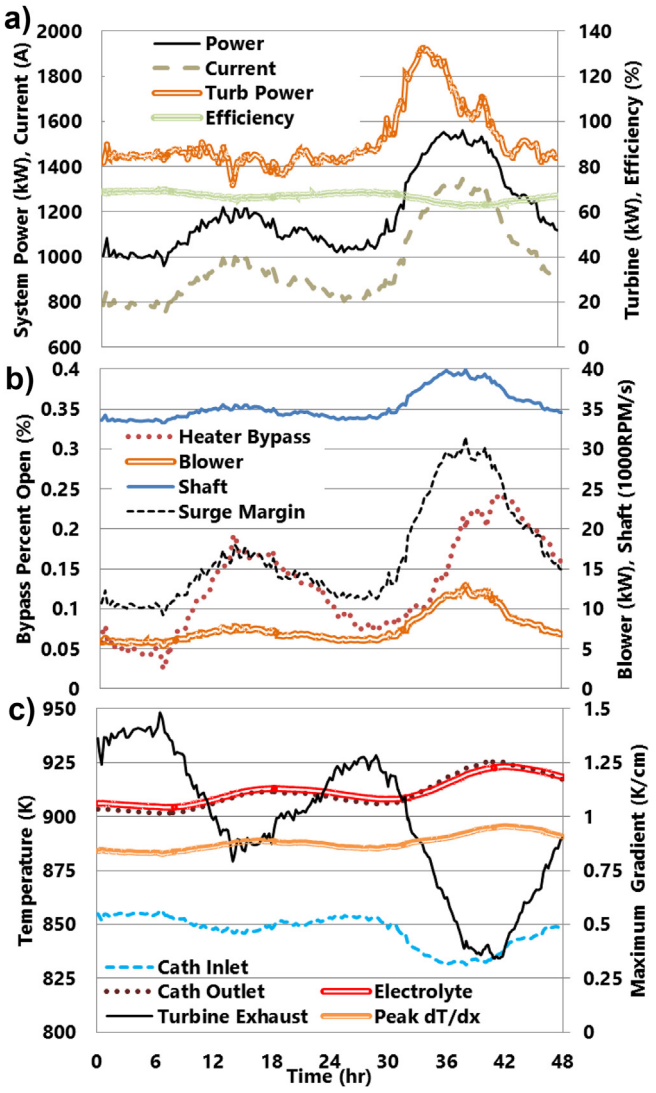

Fig. 10. Response of the FCE DFC1500®/Capstone C250® (MCFC–MTG) hybrid to a 48-h dynamic load profile using the integrated control strategy a) system power and efficiency b) control actuation c) turbo-machinery and FC temperature.

resolution of 8 × 8 enabled reasonable prediction of the local thermal gradient changes for the cross-flow configuration with indirect internal reforming utilized in the DFC-1500®. Fig. 11 details a) the spatial temperature distribution under nominal operation, b) the deviation from nominal at 12-h, c) 24-h, and d) 36-h. The cross-flow configuration results in a high temperature region near the corner where fuel is entering and air is exiting. The simulation begins at midnight, thus 12, 24, and 36 h into the simulation corresponds to noon, midnight, and the subsequent noontime. The spatial temperature profile does not vary by more than 5 °C or 8 °C at 12 and 24 h respectively, but does increase by as much as 15 °C at 36 h. The temperature increases the most in the upper left corner where fuel is entering and air is exiting, exacerbating the thermal gradient in the air flow direction. At simulation hour 36, noon on the second day, the campus is experiencing near maximum demand, 98%, and exceptionally warm ambient conditions. Both contribute to the higher thermal stress within the stack.

6. Discussion

Both non-intrusive and intrusive control techniques have been applied and evaluated for dynamic operation of hybrid SOFC-GT and MCFC–MTG systems. Non-intrusive fuel injection was capable of maintaining either cathode inlet or exhaust temperature during turndown, but not both simultaneously. The efficiency penalty for fuel injection control (either pre- or post-FC) was quite severe, and the surge margin was negatively impacted. Pre-anode fuel injection could provide benefits to stack durability and longevity, and may be necessary to control reformer characteristics in systems employing an external reformer. Inlet guide vane and speed control manipulations were found to be effective means of controlling air flow to sustain nominal stack temperature and high efficiency at part load. Reducing the air flow to the fuel cell is far more efficient than adding fuel to heat the additional air flow. The range of application for both air flow controllers is limited and increases the hybrid system likelihood of developing compressor stall/surge. Without feed-forward control, both inlet guide vane manipulation and speed manipulation exhibited unstable behavior when controlling cathode exhaust temperature due to coupling with cathode recirculation/dilution and the long thermal transient response characteristics of the high temperature fuel cell.

For the majority of the campus load following simulation the MCFC–MTG system operates between 1000 kW and 1200 kW, but the turbine produces a scant 80 kW of that total; far from the nominal 163 kW and rated 250 kW of this particular micro-turbine (if it were combustion-fired). Back-of-the-envelope type calculations suggest that the turbine-generator used in a fuel cell hybrid should be sized to meet 15–20% of the total electrical demand. If the turbine-generator could produce 250 kW it would meet 16.7% of a 1.5 MW load, indicating that the MTG used in the current turbomachinery (rated at 250 kW when combustion-fired) may actually be undersized for the current hybrid application. In operation, the turbine of this MCFC–MTG cycle produces at most 10% of the power. The performance map analysis of Part I demonstrated the significant reduction of turbine output at the reduced turbine inlet temperature. The lower operating temperature of molten carbonate technology is not able to produce turbine inlet temperatures near those of a combustor and well below those that are possible with 1000 °C SOFC technology. The reduced temperature, down to as low as 700 °C, SOFC technology that is currently being brought to commercialization is more likely to behave similar to this molten carbonate design. The 15–20% rule of thumb may still apply during the design selection phase, but the turbine-generator cannot be expected to produce anything near its combustion-rated output when integrated into these lower temperature fuel cell gas turbine hybrid systems. Gas turbines suitable for integration in hybrid systems would ideally be well sized, operate at reasonable pressure

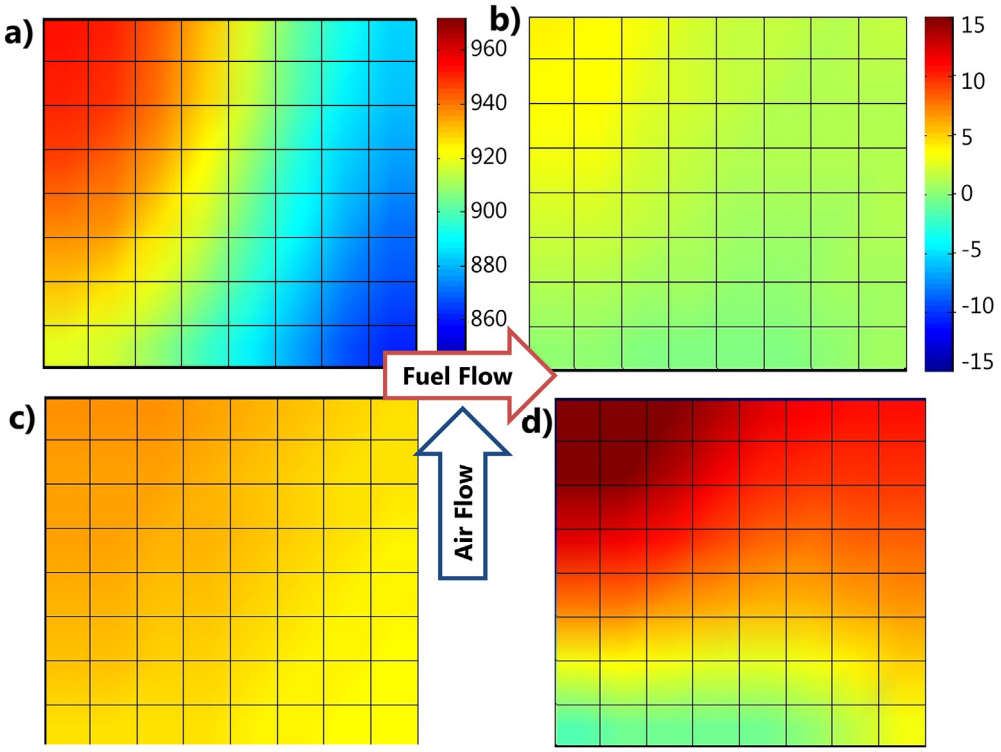

Fig. 11. Spatial temperature profile during dynamic load following simulation a) initial temperature distribution b) change in temperature distribution at 12 h c) change in temperature distribution at 24 h d) change in temperature distribution at 36 h.

ratios (3–8), include exhaust heat recuperation, and maintain a substantial surge margin over a broad range of air flow rates.

Any discrepancies between specific fuel cell heating and specific combustion heating, as defined and discussed in Part I, were accommodated through heat recuperation and cathode recirculation in the hybrid system designs. The addition of cathode recirculation intrudes upon the simple cycle integration and requires the introduction of a high temperature blower. However, cathode recirculation avoids the substantial efficiency penalty of firing a post-FC combustor to supplement the total fuel cell heating. Fuel cell bypass, introduced but not part of the final design in Part I, allows the hybrid system to balance air flow between the two subsystems and achieve a 4:1 turndown ratio. Fuel cell bypass requires a medium temperature, high pressure valve capable of bypassing air around the fuel cell and directly to the turbine.

The benchmark (existing) generation systems of a Capstone C250® and Fuel Cell Energy DFC1500® were shown amenable to integration into a 1.55 MW hybrid system with a nominal 66% LHV efficiency. A low pressure dilution blower enables dynamic load following without cathode recirculation. The blower accounts for a substantial parasitic power loss, but permits near-nominal operation of the DFC-1500® throughout a large operating envelope. Despite the six point lower nominal efficiency compared to the SOFC-GT case, the MCFC bottoming system achieves a similar overall efficiency during the 48 h transient campus load following tests; 66.7% vs. 71.1%. Both systems illustrate strong potential for dynamic load following and should be considered for further testing and demonstration as dispatchable renewable power or grid-support resources.

7. Summary and conclusions

The high temperature fuel cell gas turbine hybrid systems analyzed are two promising power generator designs. The detailed balance of plant integration necessary for the study of dynamic control systems has been used to verify the efficiencies estimated in Part I. Despite heat losses and parasitic blower loads, both the solid oxide and molten carbonate systems exhibited high fuel-to-electric efficiency at design point; 73.7% and 66.0%, respectively. The load-following simulations illustrated how thermocouples easily located in the cathode inlet and exhaust streams can be used to mitigate thermal transients in a cross-flow fuel cell with internal reformation during load transients. The simulations also demonstrated how post-FC fuel injection and compressor bleed can regain stall/surge margin in a turbine at part load. Utilizes the additional actuators described along with the simple control techniques employed, both hybrid SOFC-GT and MCFC–MTG systems were shown to operate over a wide dynamic range (between 30% and 100% of full load) while maintaining temperatures and other operating conditions within acceptable limits. These SOFC and MCFC hybrid systems are also shown to exhibit high fuel-to-electric efficiency when operating dynamically (71.1% and 66.7%, respectively) or at part load conditions (72.0% and 70.6%, respectively at 70% of full load).

Acknowledgments

The authors gratefully acknowledge the financial support of the U.S. Department of Energy under contract number 09EE0001113 to the University of California, Irvine, which provided partial support for the research presented in this paper.

References

[1] B. Tarroja, F. Mueller, J.D. Eichman, S. Samuelsen, Energy 42 (1) (2012) 546–562.
[2] M.C. Cameretti, R. Tuccillo, R. Piazzesi, Appl. Therm. Eng. 59 (1–2) (2013) 162–173.
[3] H. Ghezel-Ayagh, J. Walzak, D. Patel, J. Daly, H. Maru, R. Sanderson, W. Livingood, J. Power Sources 152 (2005 March) 219–225.
[4] F. Mueller, F. Jabbari, J. Brouwer, J. Power Sources 187 (2) (2008) 452–460.
[5] S. Samuelsen, J. Brouwer, in: J. Garche (Ed.), Encyclopedia of Electrochemical Power Sources, first ed., Elsevier Science, 2009, pp. 124–134.
[6] A. Rao, J. MacLay, S. Samuelsen, J. Power Sources 134 (2004 June) 181–184.
[7] R.A. Roberts, J. Brouwer, J. Fuel Cell Sci. Technol. 3 (2006 February) 1–7.
[8] D. Mclarty, Y. Kuniba, J. Brouwer, G. Samuelsen, J. Power Sources 209 (2012) 195–203.
[9] F. Mueller, F. Jabbari, R. Gaynor, J. Brouwer, J. Power Sources 172 (2007) 308–323.
[10] M. Ferrari, E. Liese, D. Tucker, L. Lawson, A. Traverso, A.F. Massardo, Trans. ASME (2007 October) 1012–1019.
[11] M.L. Ferrari, M. Pascenti, R. Bertone, L. Magistri, J. Fuel Cell Sci. Technol. 6 (3) (2009).
[12] M.L. Ferrari, M. Pascenti, L. Magistri, A.F. Massardo, J. Fuel Cell Sci. Technol. 7 (2) (2010).
[13] M.L. Ferrari, A.F. Massardo, Appl. Energy 105 (2013) 369–379.
[14] M.L. Ferrari, J. Power Sources 196 (5) (2011) 2682–2690.
[15] E.A. Greppi PBBa, Int. J. Hydrogen Energy 33 (2008) 6327–6338.
[16] F. Ghigliazza, A. Traverso, A.F. Massardo, J. Wingate, M. Ferrari, J. Fuel Cell Sci. Technol. (2009) 1–7.
[17] R. Roberts, J. Brouwer, E. Liese, R.S. Gemmen, in: Development of Controls for Dynamic Operation of Carbonate Fuel cell-gas Turbine-hybrid Systems. Proceedings of ASME Turbo Expo 2005, 2005, pp. 1–7. Reno-Tahoe.
[18] P. Costamagna, L. Magistri, A.F. Massardo, J. Power Sources (2001) 352–368.
[19] F. Mueller, R. Gaynor, A.E. Auld, J. Brouwer, F. Jabbari, G.S. Samuelsen, J. Power Sources 176 (2008) 229–239.
[20] A. Nakajo, F. Mueller, D. McLarty, J. Brouwer, J. Van herle, D. Favrat, J. Electrochem. Soc. 158 (2011) B1329–B1340.
[21] A. Nakajo, Z. Wuillemin, J.V. herle, D. Favrat, J. Power Sources 193 (1) (2009) 203–215.
[22] A. Nakajo, Z. Wuillemin, J.V. herle, D. Favrat, J. Power Sources 93 (1) (2009) 216–226.
[23] M. Sheng, M. Mangold, A. Kienle, J. Power Sources 162 (2006 Septempber 28) 1213–1219.
[24] C. Stiller, B. Thorud, O. Bolland, Rambabu Kandepu, L. Imsland, J. Power Sources (2006) 303–315.
[25] O. Razbani, I. Wærnhus, M. Assadi, Appl. Energy 105 (2013) 155–160.
[26] D. McLarty, J. Brouwer, S. Samuelsen, Int. J. Hydrogen Energy (2013) 1–12.
[27] L. Barelli, G. Bidini, A. . O, Appl. Energy 110 (2013) 173–189.
[28] Z. Jia, J. Sun, S.R. Oh, H. Dobbs, J. King, J. Power Sources 235 (2013) 172–180.
[29] W. Burbank, D. Witmer, F. Holcomb, J. Power Sources (2009) 656–664.
[30] R. Roberts, J. Brouwer, F. Jabbari, T. Junker, H. Ghezel-Avagh, J. Power Sources (2006) 484–491.
[31] A. Traverso, L. Magistri, A.F. Massardo, Energy 35 (2) (2009) 764–777.
[32] D.A. Brunner, S. Marcks, M. Bajpai, A.K. Prasad, S.G. Advani, Int. J. Hydrogen Energy 37 (2012) 4457–4466.